A first study on an oscillatory flow enclosed in a finite cylinder

Carles Panadès i Guinart

PhD supervisor: Francisco Marques

Departament de Física Aplicada, Universitat Politècnica de Catalunya. 08034 Barcelona, Spain.

Abstract

In this preliminar work, an oscillatory flow contained in a closed cylinder is investigated by means of spectral methods. The problem is quite related with the Stokes boundary layer and the major phenomena belong to this region. The basic flow is axisymmetric with $Z_2 \times O(2)$ symmetry that breaks into 3D when it becomes linearly unstable. For a fixed aspect ratio, $\Gamma = 2$, the locus in parameter space of the transition with the most unstable modes is obtained. Moreover, there are some indications of the location in phase space of the quasi-periodic mode that may be useful for further studies.

1 Introduction

For our own concern, there are two major reasons for analizing the onset of hydrodynamic instabilities in the oscillatory flow enclosed in a cylinder. On the one hand, it will help us to understand how a 2D basic flow becomes 3D in the unstabilizing process. On the other hand, the same system with a non-newtonian fluid is being studied and before addressing this topic deeply it would be better to gain as much knowloedge as possible from the newtonian scenario. In some cases, knowing the newtonian driving instability perfectly can be of great help to elucidate the complex fluid mechanism [1].

Some authors have devoted large efforts to study the bifurcations in systems with Z_2 spatio-temporal and $O(2)$ symmetry, because the transition from two-dimensional to three-dimensional flows is a fundamental step towards turbulence [2]. Such systems need the two-dimensional state to be time-periodic. Some examples are the flow in a rectangular cavity driven by a harmonic oscillation of one of the walls [3,4] or the periodically shedding wake of a bluff body [5], i.e. the well-known von Kármán vortex street [6]. Both systems share the same symmetries and great similarities with respect to the unstable modes. As a matter of fact, theoretical studies and numerical simulations predict the existence of two synchronous modes (A and B) and a quasi-periodic mode (QP). The two synchronous modes possess a long and a short wavelength, as well as in each case one of them preserves the spatio-temporal symmetry whilst the other does not. The QP mode manifests itself in the non-linear regime as modulated travelling waves (TW). In these calculations, a periodicity defined by a concrete wavelength is assumed in the spanwise direction. However, in experiments the apparatus usually is rather large, but finite. This is likely the reason why in the finite-span experiments, the TW nature of the quasiperiodic mode is replaced by a nonpropagating mode with spatial features similar to those of the traveling mode, meanwhile the synchronous modes existence is perfectly corroborated. Consequently, the only way of achieving real periodicity in the streamwise direction in the cavity flow is by folding the system, thus yielding to a cylindrical frame, analogously to the plane Couette and Taylor-Couette flow. In this novel system, the same phenomenology should occur and the agreement with the experiments ought to be in a better correspondance than former assays.

Let us talk about the potential interests in complex fluids. The study of an oscillatory flow in a circular cross section or in a confined cylinder can be applied in several disciplines. For example, in the industry sector it has been suggested that oscillatory flows may reduce wetting layers of viscoelastic fluids [7] and could help in the treatment of contaminated groundwater aquifers [8], while in the Biophysics field can provide a better unserstanding of the circulatory or breathing system [9]. Currently, the onset of instabilities of a complex fluid in a large aspect ratio cylinder is a question under study [10]. As a matter of fact, the flow becomes unstable for a correct choice of the parameters. However, whether the driving mechanism is purely viscoelastic or not, is still obscure [11]. Therefore, tackling the problem from a numerical point of view might be quite fruitful in unravelling the instability nature.

2 Methodology

Consider a newtonian fluid with kinematic viscosity ν confined in a finite cylinder of radius R and height h, whose lateral surface oscillates periodically providing a time-dependant boundary condition of the

z-velocity at the wall $V_{max}\sin(2\pi t/T)$, meanwhile the top and lower lids remain at rest. The system is non-dimensionalized taking R as a length scale, and the viscous time $\tau = R^2/\nu$ as a time scale, three non-dimensional parameters that completely govern the flow can be defined: the cylinder aspect ratio Γ

$$\Gamma = \frac{h}{R}\,, \tag{1}$$

the Reynolds number Re

$$Re = \frac{V_{max}R}{\nu}\,, \tag{2}$$

and the Stokes number St

$$St = \frac{R^2}{T\nu}\,. \tag{3}$$

In this preliminar study, we restrict our simulations to $\Gamma = 2$ for the sake of simplicity.

The incompressible Navier-Stokes Equations (NSE) govern the fluid dynamics:

$$\left(\frac{\partial}{\partial t} + \mathbf{u}\cdot\nabla\right)\mathbf{u} = -\nabla p + \frac{1}{Re}\nabla^2\mathbf{u} \tag{4a}$$

$$\nabla\cdot\mathbf{u} = 0 \tag{4b}$$

where $\mathbf{u} = (u, v, w)$ is the non-dimensional velocity field in cylindrical coordinates (r, θ, z), and p is the pressure.

Non-slip velocity boundary conditions are used on all walls at any time. As it has already been said, the velocity field is zero on steady walls, whilst the z-component at the lateral wall oscillates in time:

$$\mathbf{u}(r,\theta,0) = (0,0,0) \tag{5a}$$

$$\mathbf{u}(r,\theta,h) = (0,0,0) \tag{5b}$$

$$\mathbf{u}(R,\theta,z) = (0,0,V_{max}\sin(2\pi t/T)) \tag{5c}$$

Naturally, the basic flow will have the symmetries imposed by the equations with the boundary conditions. The spatial invariances are reflections about any (r, z)-plane (constant θ) and arbitrary translations in the spanwise θ-direction:

$$K(u,v,w)(r,\theta,z,t) = (u,-v,w)(r,-\theta,z,t) \tag{6a}$$

$$R_\alpha(u,v,w)(r,\theta,z,t) = (u,v,w)(r,\theta+\alpha,z,t) \tag{6b}$$

for any real α. The two operators generate the $O(2)$ symmetry group in the periodic spanwise θ-direction. The harmonic oscillation of the lateral wall introduces an additional spatio-temporal symmetry. Therefore, the system is also invariant to a reflection about the half-height plane $z = 0$ together with a half-period evolution in time:

$$H(u,v,w)(r,\theta,z,t) = (u,v,-w)(r,\theta,-z,t+T/2) \tag{7}$$

This transformation generates a Z_2 group and commutes with the $O(2)$ group. Hence, the complete symmetry group of the problem is $Z_2 \times O(2)$.

The NSE have been solved employing a second order time-splitting method [12,13]. The spatial discretization has been performed by means of a Galerkin-Fourier expansion in the azimuthal coordinate θ and Chebyshev collocation in $x = 2r$ and $y = 2z/\Gamma$, of the form:

$$F(r,\theta,z) = \sum_{l=0}^{L}\sum_{n=0}^{N}\sum_{m=M}^{M} a_{l,n,m}T_l(x)T_n(y)e^{im\theta} \tag{8}$$

where the real or imaginary parts of F are the velocity components and the pressure. The radial dependance is approximated using Chebyshev expansions with the proper parities of their azimuthal Fourier component. In order to avoid including the origin in the collocation mesh, an odd number of Gauss-Lobato points in r has been used and the equations are solved only in this interval. For each Fourier mode, the resulting Helmholtz and Poisson equations are solved utilizing diagonalization techniques in both the radial and axial directions. Just mention that the decoupling of the Helmholtz equation for u and v has been achieved by using the combinations:

$$u_+ = u + iv \tag{9a}$$

$$u_- = u - iv \tag{9b}$$

Somehow, the boundary conditions are fictitious because in the idealized scenario that is depicted, they have been considered discontinous at the junctions of the lids with the lateral wall. As a matter of fact, in the experiment there are small but finite gaps where the velocity can be adjusted to zero very rapidly. In order to provide smoothness and avoid numerical artifacts, a regularization condition ought to be applied where the lids meet the lateral wall:

$$\begin{aligned} w(R,\theta,z,t) =& A(t)\left[1-\exp\left(-\frac{1-z}{\epsilon}\right)\right]\times \\ &\times\left[1-\exp\left(-\frac{1+z}{\epsilon}\right)\right] \end{aligned} \tag{10}$$

where $A(t) = V_{max}\sin(2\pi t/T)$ is the amplitude of the velocity at a concrete time, and $\epsilon = 6\cdot 10^{-3}$ is a fixed regularization parameter.

There are several ways of checking the spectral convergence of the code. Our choice are the energies (L_2-norms) of the different modes. In integral form, the total kinetic energy is:

$$E = \frac{1}{2}\int_V \mathbf{u}\cdot\mathbf{u}^* dV \tag{11}$$

where the integral is extended in the whole volume, and the star superindex denotes the complex conjugate. An illustrative example is given by the energies

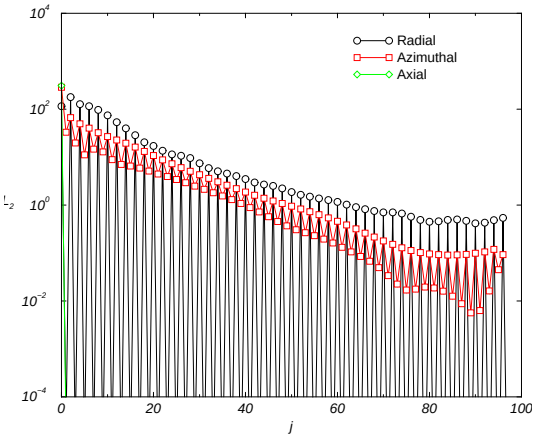

Figure 1: Detail of the convergence of the spectral coefficients of the L_2 norm. A flow at $Re = 1000$ and $St = 318.31$ has been perturbed with a $\delta \sim 10^{-4}$ and $L = 48$, $M = 10$ and $N = 96$ are considered.

of the azimuthal modes of a given solution:

$$E_m = \frac{1}{2}\int_{-1}^{+1}\int_{0}^{1} \mathbf{u}_m \cdot \mathbf{u}_m^* r dr dz \qquad (12)$$

where $\mathbf{u}_m$ is the m-th Fourier mode of the velocity field. For the remaining modes, the operations are completely analogous. Figure 1, shows the L_2-norms at $Re = 1000$ and $St = 318.31$ for a flow, whose azimuthal modes have been perturbed with a perturbation of amplitude $\delta \sim 10^{-4}$. This solution has been computed with $L = 48$ and $N = 96$ Chebyshev points in r and z, and $M = 10$ Fourier modes in θ. Note that the radial convergence is measured through x, so there are $L_x = 2L + 1$ coefficients. Since the energy coefficients for j large are two or three orders of magnitude smaller than the leading coefficients, the spectral accuracy is quite satisfactory. For a non-perturbed flow, the results are equivalent with the only difference that the azimuthal terms are all zero, except the zero mode because of the axisymmetry of the basic flow. This statement is a first prove of the symmetry breaking of the system, going from a 2D axisymmetric flow to a 3D state. Time steps of $dt = 10^{-6}$ have been required to ensure numerical stability and accuracy of the temporal scheme.

Some lines above and without prior warning, we have introduced the concept of perturbations. Before entering the turbulent stage, the two-dimensional flow may break into a new three-dimensional state. Due to some small perturbations of the basic flow, the fluid might become linearly unstable. After these perturbations have become large enough they may interact on a non-linear fashion, thus forming a new three-dimensional structure. In this preliminar study, we restrict ourselves to the linear stability analysis of the basic flow.

From a non-perturbed solution, further calculations are restarted by perturbing all the Fourier modes of the basic flow with $\delta \sim 10^{-4}$. Taking a careful look to the energy spectra, it can be observed how the Fourier modes grow or decreases linearly after some non-linear transitory. The fastest growing mode indicates which one leads the linear instability. For a fixed Stokes number, this process has been repeated for different Reynolds numbers until finding from whom the instability began. Having delimited the Reynols interval, more calculations have been carried out with a smaller perturbation ($\delta \sim 10^{-8}$) and only acting on the Fourier mode that turns to be unstable. The growth ratio of the most unstable mode before and after are computed, and the critical Reynolds is obtained straightforwardly by means of a linear interpolation because the critical point is close enough to take this consideration as valid.

3 Results

3.1 Basic State

As expected, the basic basic flow is always axisymmetric and possesses the $Z_2 \times O(2)$ symmetry. Since there is an oscillatory forcing, our problem enters the Stokes boundary layer domain. The Stokes boundary layer (or oscillatory boundary layer), refers to the boundary layer close to a solid wall in oscillatory flow of a viscous fluid. The thickness of the oscillatory boundary layer is called the Stokes boundary-layer thickness:

$$l \sim \sqrt{\frac{2\nu}{\Omega}} \qquad (13)$$

where $\Omega = 2\pi/T$. An important observation for the oscillating Stokes flow is, that vorticity oscillations are confined to a thin boundary layer and damp exponentially when moving away from the wall in the laminar or turbulent regime. Outside the Stokes boundary layer, the vorticity oscillations may be neglected. In the most paradigmatic problem related with the Stokes boundary layer, the system has an infinite length ($\Gamma \to \infty$) and the fluid profile is just $v_z(r)$. Since our system has to satisfy the NSE with the stipulated boundary conditions, a radial velocity profile appears near the lids.

Then, the most relevant magnitudes that feature the basic flow are the radial velocity, the axial velocity, the stream function and the kinetic energy. The vorticity only has aximuthal component, thus confirming that it is perpendicular to the velocity field. In Figures 2-5, these magnitudes are depicted for different Stokes and Reynolds sets at the instant where the sidewall velocity is maximum. The values for St are chosen for two reasons. Firstly, the four factor between them will help us to identify some properties of the boundary layer. Secondly, as it will be commented later on, the mode that undergoes the instability is different in each case (2 and 3, respectively). The Reynolds numbers are in such a way that each is slightly greater and

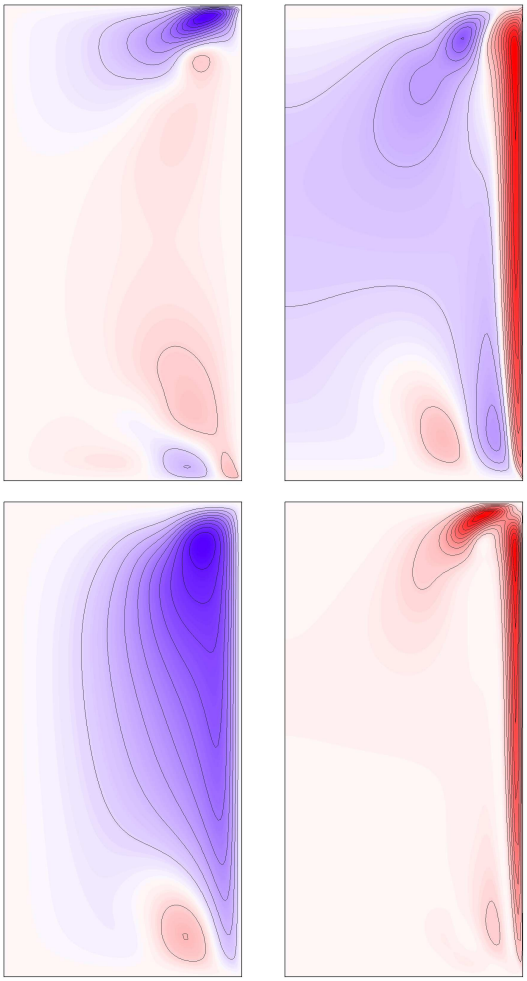

Figure 2: From left top to down right, radial velocity, axial velocity, stream function and kinetic energy for $Re = 600$ and $St = 159.15$ near the maximum of the sidewall velocity in a meridional plane, $(r, z) \in [0, 1] \times [-1, 1]$ (θ-section), in the basic state. Red (blue) corresponds to positive (negative) values.

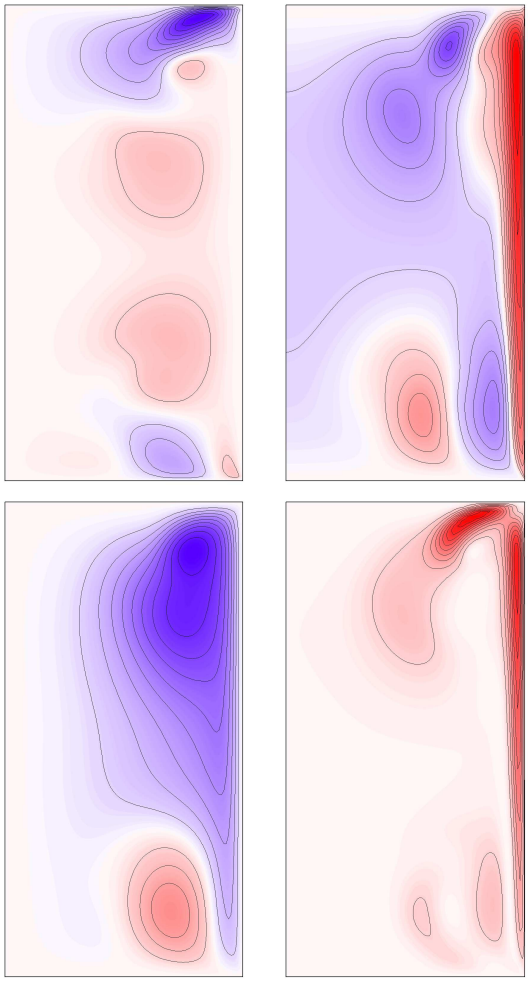

Figure 3: From left top to down right, radial velocity, axial velocity, stream function and kinetic energy for $Re = 800$ and $St = 159.15$ near the maximum of the sidewall velocity in a meridional plane, $(r, z) \in [0, 1] \times [-1, 1]$ (θ-section), in the basic state. Red (blue) corresponds to positive (negative) values.

smaller than the critical value.

In the top right part of Figures 2-5, the axial velocity is displayed. As a matter of fact, it provides us with an initial idea of l. Clearly, the factor four between the Stokes numbers, yields a factor two in the thicknesses. The increase in Re seems to give a less smoother profile, but their sizes do not change substantially.

Concerning to the radial velocity profiles (top left part of Figures 2-5), mention that the non-zero region increases with the boundary layer size and the Reynolds number. The boundary layer thickness determines the amount of fluid that collides with the cylinder lids, while the Reynolds the violence of the impact, so the size of the recirculation part in the superior part.

Due to the 2D nature of the basic flow, the stream funcion is a well-defined scalar field. The stream function can be used to plot streamlines, which represent the trajectories of particles in a steady flow. By simple inspection, it seems that the stream funtion does not vary much at all. Indeed, this magnitude is pretty useful to characterize the global dynamics of the system, and since the basic flow always behaves similarly (besides the length and velocity range), the stream function ought to be similar in most cases.

The kinetic energy (down right 2-5) serves well to synthesize what has already been commented about the radial and axial velocities, but nothing new comes to light.

3.2 Perturbed Flow and LSA

As soon as the perturbation is introduced in one of the velocity components, this is transmitted to the other fields through the coupling of the NSE. The perturbation on one mode may grow or decrease, thus indicating its linear stability. In case the perturbation

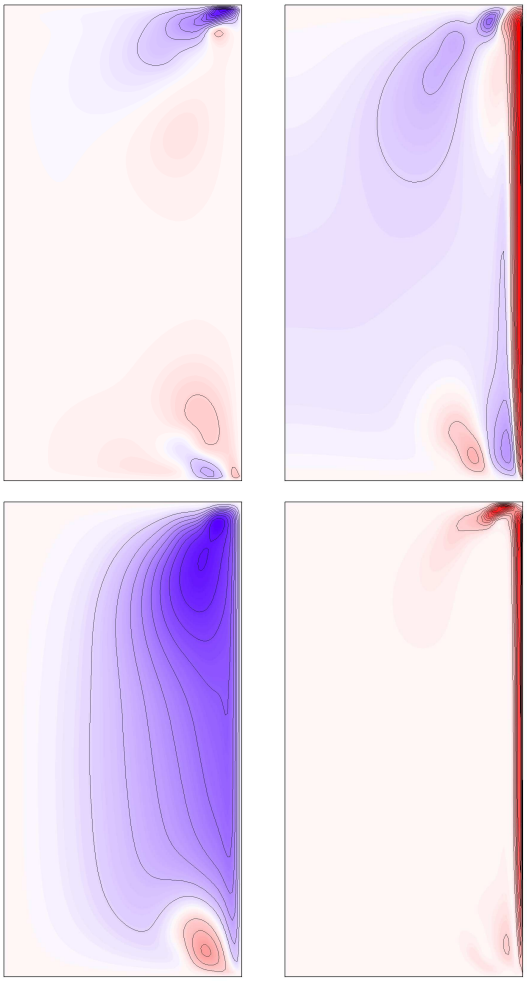

Figure 4: From left top to down right, radial velocity, axial velocity, stream function and kinetic energy for $Re = 1400$ and $St = 636.62$ near the maximum of the sidewall velocity in a meridional plane, $(r, z) \in [0, 1]\times[-1, 1]$ (θ-section), in the basic state. Red (blue) corresponds to positive (negative) values.

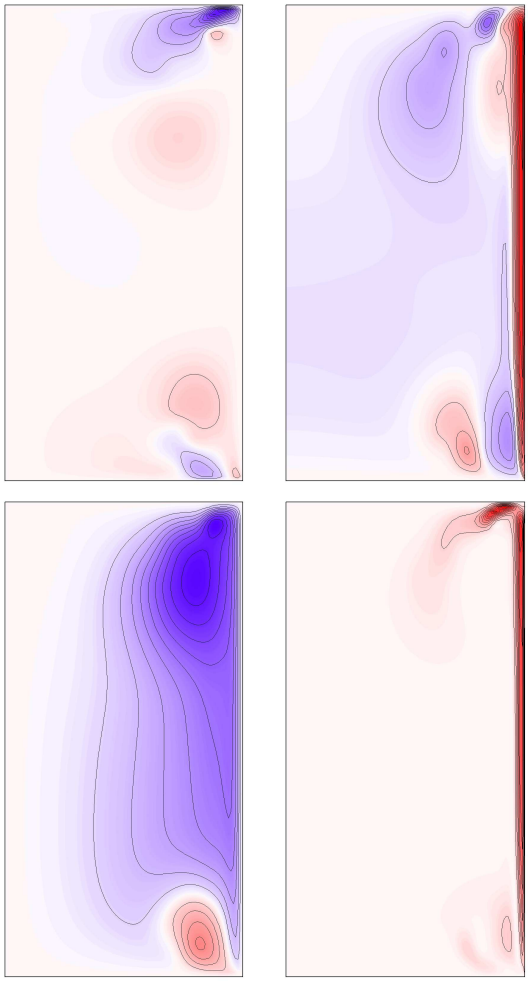

Figure 5: From left top to down right, radial velocity, axial velocity, stream function and kinetic energy for $Re = 1600$ and $St = 636.62$ near the maximum of the sidewall velocity in a meridional plane, $(r, z) \in [0, 1]\times[-1, 1]$ (θ-section), in the basic state. Red (blue) corresponds to positive (negative) values.

grows the system breaks in 3D. The linear stability analysis (LSA) has been done using direct numerical simulations, resulting in Figure 6.

Regarding to the fastest growing modes that might induce the instability, we can only speak about the computed values. For instance, from $St \in [39.79, 318.31]$ it is mode 2, $St \in [477.46, 795.77]$ mode 3, and $St = 954.93$ mode 4. Actually, the critical Reynolds for $St = 795.77$ is almost the same and, consequently, indicating that we are pretty close to the merging point of the neutral curves of modes 3 and 4. These points are very important for having codimension 2 and is a question to be tackled later on. The neutral curves have been obtained through splines.

Lastly, just mention a curiosity that could be useful for future studies. For $St = 79.58$, one of the growing modes shows the typical growth, but with another well-defined period that has nothing to do with the basic flow. This appearance might be related with the QP mentioned in the Introduction.

4 Conclusions and Perspectives

The basic flow and the subsequent destabilization of a newtonian fluid confined in an oscillating cylinder have been inestigated. As a matter of fact, the basic flow is axisymmetric with a $Z_2 \times O(2)$ symmetry group that breaks at the onset of the appearance of a new 3D flow.

The breaking of the 2D symmetry into a 3D structure usually is related with the necessity of the system to adapt to the new energy scales. In our system, the major physics are concentrated on the boundary layer and this is the location where the instabilities develop. Thus, by reducing the Stokes boundary layer size, greater energies (Reynolds numbers) are needed to make the system become unstable. In further sim-

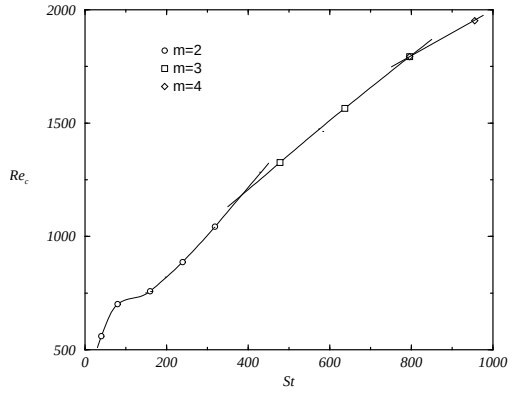

Figure 6: Critical Reynolds number Re_c, as a function of the Stokes number St. The points have been obtained by numerical calculations and merged using splines.

ulations, with the proper changes, we should look for the existance of the synchronous (A and B) and quasi-periodic modes (QP), as well as what kind of bifurcation does the system undergo (allegedly a normal pitchfork, a pitchfork of revolution, or a Neimark-Sacker bifurcation). In order to obtain more information for these modes, large-computational calculations increasing the Fourier modes would be desirable.

Future studies ought to focus on unravelling the full phase diagram, i. e. finding the curve $Re_c(St, \Gamma)$, as well as the corresponding fastest growing mode for the same parameters, $m(St, \Gamma)$. Of course, the number of spectral points will depends on the aspect ratio because intuitively $N \sim \Gamma L$ has to be satisfied. In the same way, it would be a great asset to know the instability nature for the full parameter space.

References

A. N. Morozov and W. van Saarlos, An introductory essay to subcritical instabilities and the transition to turbulence in visco-elastic parallel shear flows, Physics Reports **447**, 112-143 (2007).

F. Marques *et al*, Bifurcations in systems with Z_2 spatio-temporal and $O(2)$ spatial symmetry, Physica D **189**, 247-276 (2004).

H. M. Blackburn and J. M. Lopez, The onset of three-dimensionl standing and modulated travelling waves in a periodically driven cavity, J. Fluid Mech. **497**, 289-317 (2003).

J. J, F. Leung *et al*, Three-dimensional modes in a periodically driven elongated cavity, Phys. Rev. E **71**, 026305 (2005).

H. M. Blackburn *et al*, Symmetry breaking of two-dimensional time-periodic wakes, J. Fluid Mech. **522**, 395-411 (2005).

M. van Dyke, An album of fluid motion (Parabolic Press, 1982).

E. Corvera-Poiré *et al*, U. S. Patent No. 20050028971 (1994)

A. A. Lambert *et al*, Optimal behavior of viscoelastic flow at resonant frequencies, Phys. Rev. E **70**, 056302 (2004).

A. C. T. Aarts and G. J. Ooms, Net flow of compressible viscous liquids induced by travelling waves in porous media, J. Eng. Math. **34**, 435 (1998).

M. Torralba *et al*, Measurements of the bulk and interficial velocity profiles in oscillating Newtonian and Maxwellian fluids, Phys. Rev. E **72**, 016308 (2005).

M. Torralba *et al*, Instabilities in the oscillatory flow of a complex fluid, Phys. Rev. E **75**, 056307 (2007).

J. M. Lopez *et al*, An efficient spectral-projection method for the Navier-Stokes equations in cylindrical geometries, J. Comp. Phys. **176**, 384-401 (2002)

I. Mercader *et al*, An efficient spectral code for incompressible flows in cylindrical geometries, Computers and Fluids (accepted for publication)